

Cite this: *Dalton Trans.*, 2021, **50**, 4819Preparation of organocobalt(III) complexes *via* O₂ activation†Mads Sondrup Møller,  Jacob Kongsted  and Christine J. McKenzie *

The coupling of selective C–H activation with O₂ activation is an important goal for organic synthesis. New experimental and computational results, along with the results from experimental work accumulated over many decades, now unequivocally link O₂ activation with C–H activation by the classic Co(salen) complexes. A common holistic mechanistic framework can rationalise the formation of ostensibly diverse peroxy, superoxy, organo and alkoxide complexes of Co^{III}(salen). DFT calculations show that cobalt(III) superoxy, dicobalt(III)peroxy and cobalt(III)hydroperoxy complexes are all viable intermediates as participants in hydrogen atom transfer reactions, whereas a Co(IV)oxo intermediate is unlikely. The reaction conditions will determine the pathway followed and all pathways are initiated through the initial formation of a superoxy complex, Co^{III}(salen)(O₂)(MeOH) (EPR: $g = 2.025$, $A = 19$ G). Organo and alkoxide ligands are derived from solvent media and the trends in reactivity reveal that combination of the pK_a and BDE of the C–H of the respective solvent substrates are important. These data explain why landmark, structurally characterized, μ_2 - η^1, η^2 -peroxide and η^1 -superoxide Co(salen)–O₂ adducts were predominantly isolated from solvents with high C–H pK_a values (DMSO, DMF, DMA).

Received 19th February 2021

Accepted 15th March 2021

DOI: 10.1039/d1dt00563d

rsc.li/dalton

Introduction

Organocobalt complexes have been widely studied for at least six decades in the context of models for vitamin B₁₂. They are prepared by the reaction of Co(I) complexes with iodoalkanes, Co(III)halides with Grignard reagents,¹ and, more rarely, by the carbonylation of aliphatic alcohols with Co(II) and Co(III) precursors using CO.² Sporadic reports also document formation of organocobalt complexes without identifiable pathways.^{3,4} For example, half a century ago Cesari *et al.*⁵ described the crystal structures of Co^{III}(salen) (salen = *N,N'*-bis(salicylidene) ethylenediamine) complexes containing C-coordinated cyanomethylene and acetyl ligands which were derived from the solvents acetonitrile and acetone, respectively. In a subsequent patent they recognised that O₂ had been important for the preparations but no mechanism was suggested.⁶ Around the same time Schaefer *et al.* reported the structural characterization of landmark biomimetic Co^{III}(salen)–O₂ adducts^{7,8} that have served as important models for O₂ binding as either superoxido or peroxido ligands in heme and non-heme enzymes. In this work they also happened upon a Co^{III}(3F-

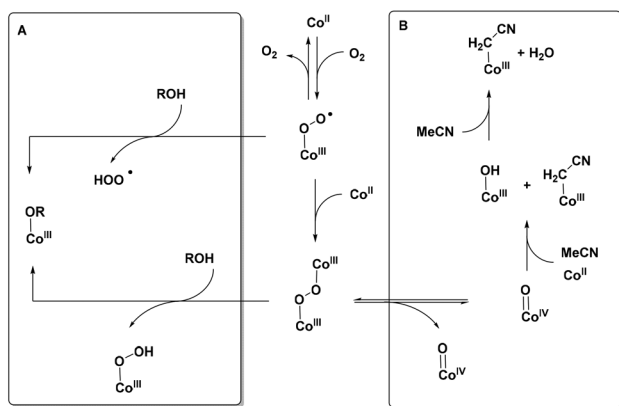
salen)-acetyl complex⁹ (3F-salen = *N,N'*-bis(3-fluorosalicylidene)ethylenediamine) when attempting to prepare an oxygenated complex directly from Calvin's original sample of Co^{II}(3F-salen)(OH₂) prepared two decades earlier.¹⁰ In parallel with this work, Nishinaga *et al.*¹¹ proposed that the formation of Co^{III}(salen) alkoxides (and hydroxides), which occurs in the presence of air in reactions of Co²⁺ and salen, includes a Hydrogen Atom Transfer (HAT) from the alcohol OH group to superoxide or peroxide complexes as depicted in Scheme 1A.

Recently Tilley and co-workers¹² proposed an O₂ activation pathway for the formation of organometallic cobalt(III) complexes of a planar tetranionic diamidodiphenol ligand, [Co^{III}(BrHBA-Et)(CH₂CN)]²⁻ (BrHBA-Et = *N,N'*-(ethane-1,2-diyl)bis(5-bromo-2-hydroxybenzamide) where the cyanomethylene ligand is derived from the acetonitrile solvent. This involves HAT from the MeCN C–H bond to a putative high-valent Co(IV)oxo complex derived from the homolytic Co–O–O–Co cleavage of an undetected μ -peroxido complex precursor. To rationalise the greater than 50% yields, a deprotonation of MeCN by an intermediate Co(III) hydroxide was invoked (Scheme 1B). It was suggested that this mechanism might be relevant also for the similar reactivity observed for the landmark Co(salen) complexes.

Scheme 1 illustrates the relationship between the aforementioned mechanistic proposals for HAT from substrate O–H or C–H bonds to Co(III)-superoxide, Co(III)₂-peroxide and Co(IV)-oxide intermediates as steps in the synthesis of Co(III)alkoxides/hydroxides/organo complexes *via* the O₂ activation by cobalt(II) complexes.

Department of Physics, Chemistry and Pharmacy, University of Southern Denmark, Campusvej 55, 5230 Odense M, Denmark. E-mail: mckenzie@sdu.dk

† Electronic supplementary information (ESI) available: Synthesis, crystallography, photolytic experiment, computational methods, IR, NMR, TGA. CCDC 2045576–2045584. For ESI and crystallographic data in CIF or other electronic format see DOI: 10.1039/d1dt00563d



Scheme 1 The relationship between the mechanisms proposed by Nishinaga *et al.*¹¹ (A) and Nguyen *et al.*¹² (B) for the O₂ dependent formation of Co^{III}(OR) complexes of salen and the Co^{III}(CH₂CN) complex of Br⁻HBA-Et. For simplicity overall charge is not depicted but it should be noted that the salen complexes in A are neutral and the complexes of Br⁻HBA-Et in B are dianionic.

We have reinvestigated the preparation of organo, alkoxide and nitrito/nitro cobalt(III) complexes of the classic unsubstituted Co(salen) scaffold using a range of solvent substrates with C–H/O–H groups. On the basis of the reaction conditions, the greater than 50% yields, spectroscopic evidence of a Co(III) superoxo intermediate and DFT calculations, we can now propose a common mechanistic framework for the formation of organo, O₂^{•-}, O₂²⁻, and alkoxide, complexes of Co(salen). This involves consecutive O₂ and C–H activations and can use Co(III)superoxide, Co(III)peroxide and Co(III)hydroperoxide intermediates in alternative pathways. We find no support for the participation of a Co(IV)oxo complex in the role of H atom acceptor.

Results and discussion

Exposure of solutions of Co(salen) dissolved in nitromethane, trifluoroethanol, acetone/methanol, acetophenone/methanol and acetonitrile/methanol to air results in colour changes from reddish-orange to emerald green or brown and Co(salen)(CH₂NO₂), Co(salen)(OCH₂CF₃), Co(salen)(CH₂COCH₃), Co(salen)(CH₂COPh) and Co(salen)(CH₂CN) are isolated respectively in yields between 50–70%. Without MeOH as co-solvent in the reactions with acetone, acetophenone and acetonitrile, the organometallic complexes are not formed. Reactions are accelerated by bubbling pure oxygen (1 atm) through the mixtures. In air, a red alkoxide and a brown nitro complex of Co^{III}(salen) were isolated from reactions in 2,2,2-trifluoroethanol and nitroethane respectively. The source of the nitrite in the latter, Co(salen)(NO₂), which was isolated in a 40% yield, is at present unknown. There are two possibilities, (i) that the solvent was contaminated by nitrite or (ii) that the nitrite ligand is formed *via* an organometallic pathway akin to the pathway described below for the formation of the remaining complexes.

For simplicity in the following molecular-level discussions, it should be noted that the aforementioned formulae represent the core Co(salen)(L) formulation where the L is derived from the solvent substrate. In each case crystallography showed the Co(III) ion is hexacoordinate, binding either an axially coordinated O-coordinated methanol or water or by forming classic M(salen) dimers where interdimeric Co...O_{Ph-salen} bonds fill the axial position. For two of the compounds, Co(salen)(CH₂COCH₃) and Co(salen)(NO₂), both monomeric and dimeric phases were structurally characterized (Fig. 1 and ESI Fig. S9, S10†). Thermogravimetric analysis (TGA) of bulk [Co(salen)(NO₂)₂·(EtNO₂)]₂ revealed the mass equivalent loss of one EtNO₂ per two Co(salen)(NO₂) at 110 °C. Further heating to 230 °C resulted in a second mass loss corresponding to one NO₂ per Co(salen). TGA on bulk Co(salen)NO₂(H₂O) showed the mass equivalent loss of one water molecule per Co(salen) at 122 °C (ESI Fig. S1†).

Crystal structures

[Co(salen)(CH₂NO₂)₂·(2MeNO₂), Co(salen)(CH₂COCH₃)(MeOH),⁵ Co(salen)(CH₂COCH₃)(H₂O), [Co(salen)(CH₂COCH₃)₂·(C₆H₆), [Co(salen)(CH₂COPh)]₂ and [Co(salen)(CH₂CN)]₂·(C₆H₆), [Co(salen)(OCH₂CF₃)₂·(4CF₃CH₂OH) and Co(salen)(NO₂) are shown in Fig. 1. Co(salen)(NO₂) occurs in two phases, one containing the dimer and the other a monomer, [Co(salen)(NO₂)₂·(EtNO₂)]₂ and Co(salen)(NO₂)(H₂O), respectively. Another phase of Co(salen)(CH₂CN) with a 1D coordination polymer structure is known.⁵

All the complexes show octahedral Co centres (Fig. 1), consistent with the +3 oxidation state and with angles deviating by an average of 0.03° from 90°. As expected, the salen ligand is almost planar in the monomeric complexes with the planes of the phenol rings twisted 8.15°, 6.44° and 5.21° from each other in Co(salen)(CH₂COCH₃)(MeOH), Co(salen)(CH₂COCH₃)(H₂O), Co(salen)(NO₂)(H₂O) respectively. All Co–C bonds lie

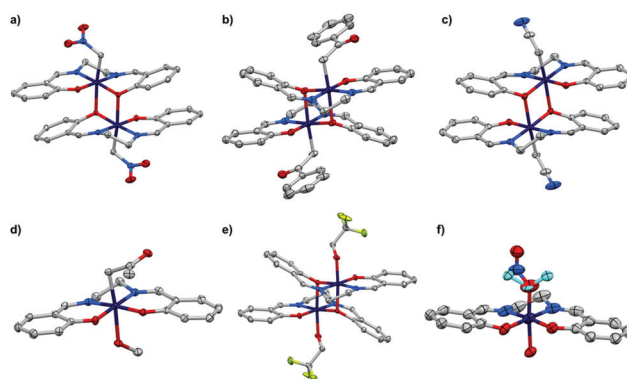


Fig. 1 Selected crystal structures. (a) [Co(salen)(CH₂NO₂)₂·(2MeNO₂), (b) [Co(salen)(CH₂COPh)]₂, (c) [Co(salen)(CH₂CN)]₂·(C₆H₆), (d) Co(salen)(CH₂COCH₃)(MeOH), (e) [Co(salen)(OCH₂CF₃)₂·(4CF₃CH₂OH), (f) Co(salen)(NO₂)(H₂O). The nitrite ligand in Co(salen)(NO₂)(H₂O) is disordered between nitro and nitrito coordination, the minor component is coloured cyan. Thermal ellipsoids are drawn at 50% probability for a–e and at 30% probability for f, H atoms and non-coordinating solvate molecules are omitted for clarity.

within the range of 1.97 Å to 2.00 Å, similar to those found earlier for related compounds.^{13,14} The dimeric structures show two different Co–O_{phenol} bond lengths, the longer bond to the μ-O ranging from 1.924–1.938 Å in the extremes of [Co(salen)(CH₂COCH₃)₂·(C₆H₆)] and [Co(salen)(NO₂)₂·(EtNO₂)] and the shorter Co–O bond to the terminal phenolato oxygen atom (1.880–1.893 Å). Characteristically¹⁵ the salen ligand deviates more from planarity in the dimeric complexes. The angles between the planes of the phenol rings range from 15.29–23.10°.

Spectroscopic characterisation

IR spectra show that the salient bands for the functional groups in the C-coordinated ligands are shifted towards lower wavenumbers compared to the parent organic molecules (Fig. 2 and Table 1). Such a shift towards lower wavenumbers might be expected to be associated with an increase in bond length, but in this case the relevant bond lengths of the parent organic molecules are virtually identical to those of the coordinated species (Table 1).¹⁶ Two bands at 1632 cm⁻¹ and 1622 cm⁻¹ in the IR spectrum of Co(salen)(CH₂COPh) are due to aromatic C=C stretching and confirm the presence of an additional phenyl group. Accordingly (due to lack of phenyl

group in axial co-ligand), only one C=C stretch appears in the spectra of the other complexes.

The crystal structures do not show any significant intra- or intermolecular interactions and the differences in the positions of the bands for the nitro, carbonyl and nitrile groups of the ligated *vs.* free species are of such large magnitude that intermolecular interactions can be ruled out as being the main cause. The decrease in band position in the organometallic complexes is, therefore, most likely related to the inductive effect of the group being coordinated to Co(III).

In the ¹H NMR spectra, the signals for the protons of the coordinating methylene groups are shifted downfield compared with the corresponding methyl signals of the parent solvents. For instance, these appear at 2.88 ppm in the spectrum of Co(salen)(CH₂COCH₃) compared to 2.08 ppm for acetone (Fig. 3a). In contrast the distal acetyl methyl group signal is shifted upfield to 1.64 ppm. Reminiscent of the changes in the IR spectra, these field shifts could be due to the inductive effect of the highly charged Co(III) ion.^{1,18} While the coordinated methylene group protons can be identified in ¹H NMR spectra, the carbon resonances of the coordinating methylene groups (C_c) are not apparent in the ¹³C NMR spectra (*e.g.* Fig. 3b). The explanation for this is that the carbon is bonded directly to the quadrupole nucleus ⁵⁹Co (100% abundance, *I* = 7/2, *Q* = 0.42) and the *T*₁ relaxation is too fast to allow detection of the coupling. In addition, residual line broadening¹⁹ means that in practice the signal for the coordinated carbon is undetectable. Although we cannot find this explicitly stated anywhere in the literature, presumably this is the reason that Co–C complexes have, to date, been characterised only by solution-state ¹H NMR spectroscopy.

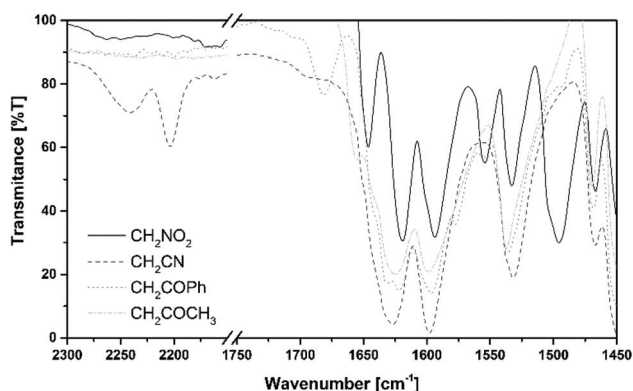


Fig. 2 ATR-FT IR spectra of [Co(salen)(CH₂NO₂)₂·(MeNO₂)], Co(salen)(CH₂COCH₃)(MeOH), [Co(salen)(CH₂COPh)]₂ and Co(salen)CH₂CN.

Table 1 Selected vibrational frequencies and bond lengths for the organocobalt and the solvent molecules from which they are derived

Compound	Group	ν_{group} [cm ⁻¹]	Bond length (group) [Å]
Co(salen)(CH ₂ NO ₂)	NO ₂	1496	1.229(7)
CH ₃ NO ₂		1570 ^a	1.21(2) ^b
Co(salen)(CH ₂ COCH ₃)	C=O	1655	1.228(4)
(CH ₃) ₂ CO		1720 ^a	1.22(3) ^b
Co(salen)(CH ₂ COPh)		1681	1.229(2)
CH ₃ COPh		1702 ^a	—
Co(salen)(CH ₂ CN)	C≡N	2204	1.151(3)
CH ₃ CN		2258 ^a	1.157 ^b

^a IR stretches for solvents obtained from NIST.¹⁷ ^b Bond lengths for solvents obtained from Sutton *et al.*¹⁶

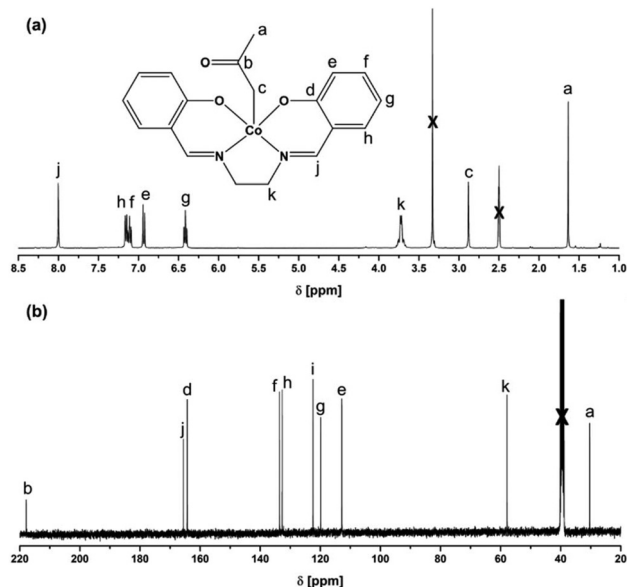


Fig. 3 (a) ¹H NMR spectrum (d₆-DMSO) and (b) ¹³C NMR spectrum of Co(salen)(CH₂COCH₃)(MeOH) with assignments. Residual solvent peaks and H₂O are marked with X.

We turned, therefore, to solid-state ^{13}C CPMAS NMR spectroscopy and found that the coordinating methylene groups of the organocobalt complexes can be identified. The signals are however relatively broad due to poorly resolved coupling to the $I = 7/2$ Co nucleus (Fig. 4a and b). The signal at 19.1 ppm and the shoulder at 48.5 ppm are assigned to this group in the ^{13}C CPMAS NMR spectra of $\text{Co}(\text{salen})(\text{CH}_2\text{COCH}_3)(\text{H}_2\text{O})$ and $[\text{Co}(\text{salen})(\text{CH}_2\text{NO}_2)]_2 \cdot (2\text{MeNO}_2)$ respectively. Comparison of the integrals of these peaks with those of the ethylene backbone gives salen : $\text{CH}_2\text{C}(\text{O})\text{CH}_3$ and salen : CH_2NO_2 ratios of 1 : 1, as expected. The resonances for the coordinating carbon atoms are shifted approximately 10 ppm upfield compared to the corresponding carbon atoms of the methyl groups in MeNO_2 and acetone (62.6 ppm and 30.6 ppm respectively), consistent with the coordinated carbon being more shielded. Curiously, this can be contrasted to the downfield shifts observed for the protons attached to these coordinated methylene carbon atoms found in the solution state ^1H NMR spectra. These observations, in the complementary NMR and IR spectra, are

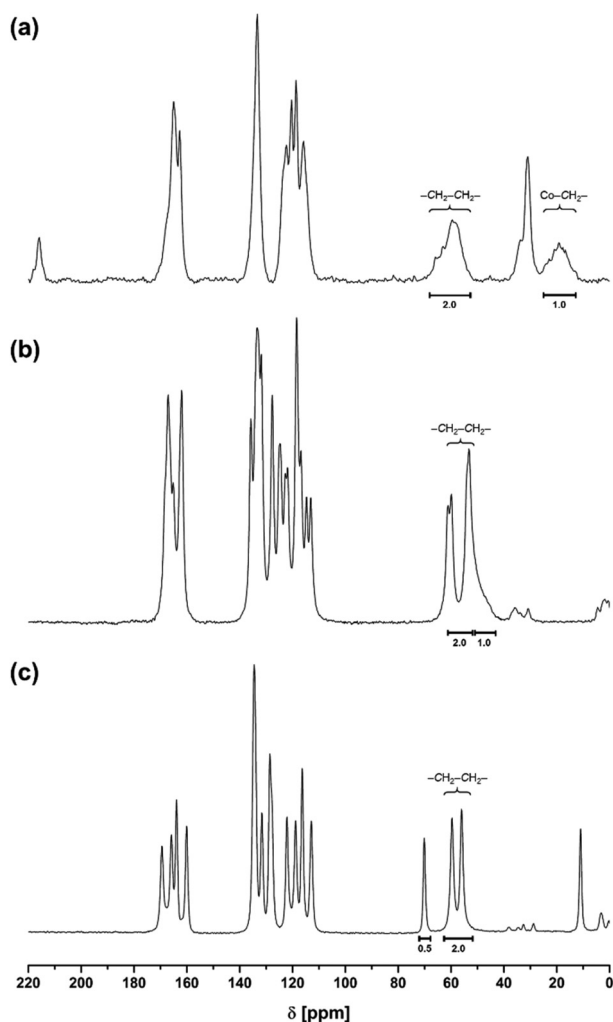


Fig. 4 ^{13}C CPMAS NMR spectrum of (a) $[\text{Co}(\text{salen})(\text{CH}_2\text{COCH}_3)(\text{H}_2\text{O})]$ (b) $[\text{Co}(\text{salen})(\text{CH}_2\text{NO}_2)]_2 \cdot (\text{MeNO}_2)$ and (c) $[\text{Co}(\text{salen})\text{NO}_2]_2 \cdot (\text{EtNO}_2)$.

consistent with the electrons in the C-coordinated ligand being delocalised towards the coordinating carbon atom and the cobalt atom. The resonances at 216.0 and 31.0 ppm in the spectrum of $\text{Co}(\text{salen})(\text{CH}_2\text{COCH}_3)(\text{H}_2\text{O})$ are due to the carbonyl and methyl group of the coordinated acetylonyl respectively. A resonance at 61.3 ppm in the spectrum of $[\text{Co}(\text{salen})(\text{CH}_2\text{NO}_2)]_2 \cdot (2\text{MeNO}_2)$ is assigned to equimolar co-crystallised MeNO_2 , consistent with TGA results (Fig. S1, ESI †). The solid-state ^{13}C CPMAS NMR spectra also reveal the subtle environment differences that are lost on dissolution when compared with the solution-state spectra. To illustrate this, the spectrum of $[\text{Co}(\text{salen})(\text{NO}_2)]_2 \cdot (\text{CH}_3\text{CH}_2\text{NO}_2)$ (Fig. 4c) shows four resonances for the four crystallographically distinct imine carbons in the region 175–155 ppm and two signals for the phenoxy carbons as is consistent with the dimeric structure. By comparison there are only two imines (134.34, 133.94 ppm) in the solution state (Fig. S20, ESI †). Resonances at 60.0 ppm and 56.0 ppm belong to the ethylene backbone in contrast to one at 58.02 ppm in solution (Fig. S20, ESI †).

The resonances at 70.1 ppm and 11.0 ppm are assigned to the co-crystallised EtNO_2 solvate and the integrals indicate a salen/ EtNO_2 ratio of 2 : 1, entirely consistent with TGA measurements on $[\text{Co}(\text{salen})(\text{NO}_2)]_2 \cdot (\text{CH}_3\text{CH}_2\text{NO}_2)$ (Fig. S1, ESI †).

Photolability

The homolytic cleavage of the Co–C bond in $\text{Co}(\text{salen})(\text{CH}_2\text{COCH}_3)$ to regenerate $\text{Co}(\text{salen})$ and an acetylonyl radical is, not unexpectedly,²⁰ induced by light. Time-resolved UV-vis spectroscopy (Fig. 5) shows that the absorption bands, most noticeably those at 354 nm and 784 nm, disappear over a few minutes on irradiation (365 nm). A radical trapping experiment was carried out by exposing a d_6 -DMSO solution of $\text{Co}(\text{salen})(\text{CH}_2\text{COCH}_3)$ (7.8 mM) and (2,2,6,6-tetramethylpiperidin-1-yl)oxyl (TEMPO) (62.4 mM) to light for 48 h at ambient temperature. A colour change from brownish green to

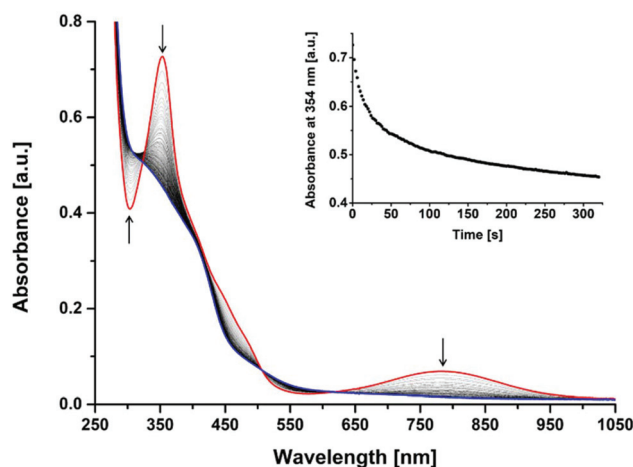


Fig. 5 Photoinduced homolytic cleavage of Co–C bond in $\text{Co}(\text{salen})(\text{CH}_2\text{COCH}_3)$ (0.1 mM, DCM) to afford $\text{Co}(\text{salen})$ and $\text{CH}_3\text{COCH}_2^\cdot$ using a 365 nm LED.

red over this time indicated the formation of Co(salen) (Fig. S3, ESI†). ^1H NMR spectra (Fig. 5) before and after irradiation show that the characteristic signals around 3.9 ppm, corresponding to the ethylene backbone of Co(salen)(CH₂COCH₃) disappear, consistent with cleavage of the Co–C bond to produce the paramagnetic (NMR invisible) Co(II) species (Fig. 6). The acetyl radical was trapped to form TEMPO–CH₂COCH₃, as evidenced by a signal at $\delta = 4.4$ ppm corresponding to the methylene protons in the NMR spectrum. This shows also that acetone is generated and this might be occurring by H atom transfer to the acetyl radical by PCET from a Co^{II}(salen) water complex. The ESI mass spectrum of the mixture shows Co(salen) and TEMPO–CH₂COCH₃ (Fig. S5†).

Spectroscopic detection of superoxide intermediate

Time-resolved UV-visible spectroscopy shows that conversion of Co(salen) to Co(salen)(CH₂NO₂) in degassed nitromethane takes approximately 48 hours after exposure to air at ambient temperature. There is no sign of an intermediate in the time-resolved UV-vis spectra (Fig. S6†). However, if the reaction is carried out in acetone/methanol (3 : 2 v/v) while purging with O₂, after approximately 15 minutes an intermediate is detected using EPR spectroscopy (Fig. 7a). In turn, this signal disappears as the species is converted over the course of 45 minutes ($t_{1/2} \approx 22$ min) to the carbon-coordinated product (Fig. 7b). The signal shows that the intermediate is a $S = 1/2$ species with hyperfine coupling to a ^{59}Co ($g = 2.025$, $A = 19$ G). This is assigned to the η^1 -superoxo complex Co(salen)(O₂[•]) (MeOH). The g -value and hyperfine coupling constant are similar to those previously reported for this well-known class of compound.²¹

An axial MeOH ligand is included in the formulation because the C–H activation reaction of acetone, acetophenone or acetonitrile does not occur in the absence of MeOH as a co-solvent. Calculations of the g -value for the structures without, or with, axial solvent ligands *i.e.*, Co(salen)(O₂[•]), Co(salen)(O₂[•])(CH₃)₂CO and Co(salen)(O₂[•])(MeOH), gave $g = 1.9675$, 1.9593

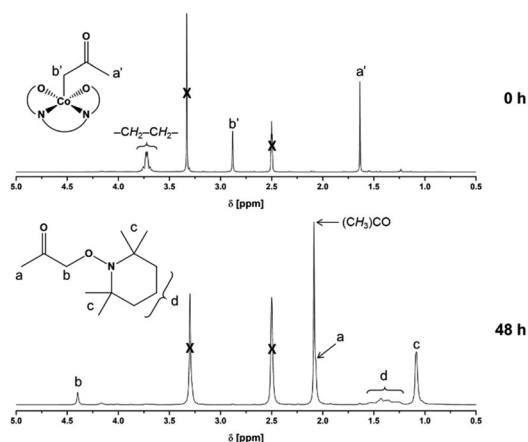


Fig. 6 ^1H NMR spectra (d_6 -DMSO) of Co(salen)(CH₂COCH₃) and TEMPO before and after visible light irradiation at room temperature for 48 hours. Residual solvent peaks are marked with X.

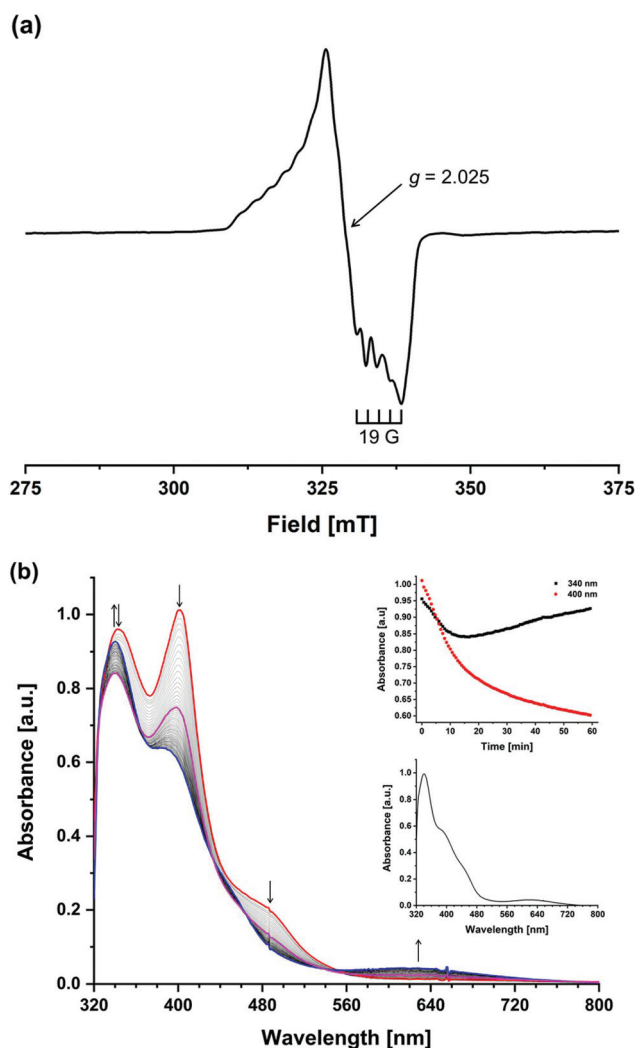
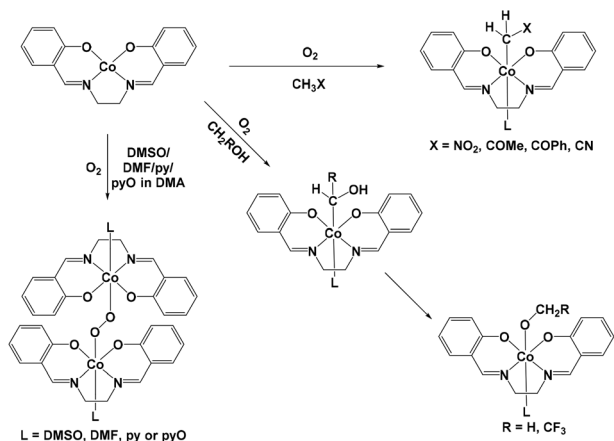


Fig. 7 (a) EPR spectrum of a solution of Co(O₂)(salen) (acetone/methanol, 100 K, microwave frequency 9.30858 GHz). (b) Time-resolved conversion of Co(salen) (0.1 mM) to Co(salen)(CH₂COCH₃) at 20 °C upon its reaction with O₂ in a degassed solution of acetone/methanol (3 : 2). Red trace is Co(salen), blue trace is $t = 60$ min, magenta trace is $t = 15$ min. Insert bottom: UV-vis spectrum of independently prepared Co(salen) (CH₂COCH₃) in acetone/methanol (3 : 2).

and 1.9921, respectively, from which it is seen that the predicted g -value for Co(salen)(O₂[•])(MeOH) is nearest the measured value. Even more importantly, mechanistic DFT calculations show that Co(salen)(O₂[•])(MeOH) is the more stable of the three possibilities (see details below). These results concur with the formation of the Co(III)superoxo complex Co(salen)(O₂[•])(MeOH), and the observations are furthermore entirely consistent with the proposal of a superoxo complex by Nishinaga *et al.*²² as the crucial intermediate prior to the formation of cobalt(III)peroxyquinolato complexes when a Co(II) complex of a pentadentate diamine ligand related to salen was reacted with 2,6-di-*tert*-butylphenols in the presence of O₂.

Peroxo-bridged Co^{III}(salen) complexes have been isolated from DMSO, DMF, pyridine and dimethylacetamide (DMA).²³



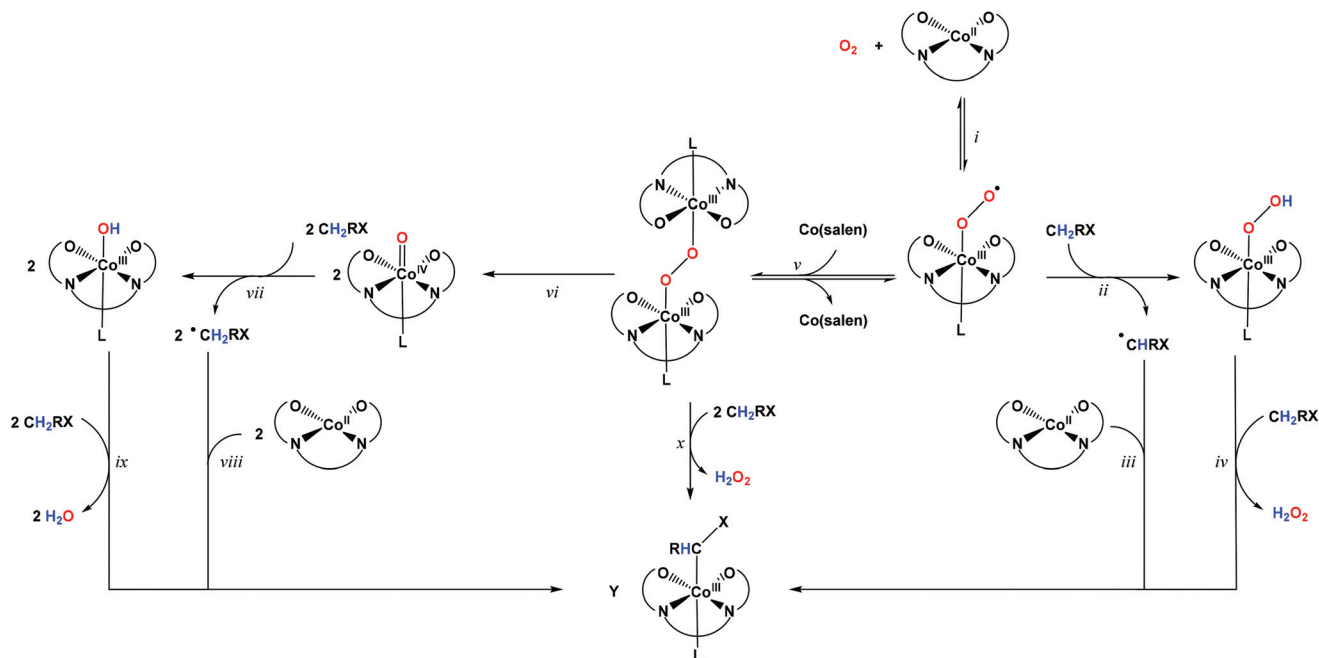
Scheme 2 The products of reactions of Co(salen) when exposed to oxygen in different solvents. X = NO₂, COCH₃, COC₆H₅ and CN. L = DMSO, DMF, py, pyO.²³ L are the second axial ligands found in the crystal structures and important for the solution state O₂ activation. These are solvent-derived or a phenolato O atom from the other complex in a dimer.

These form by reactions of Co^{II}(salen) with O₂ and along with the reactions described above, are depicted in Scheme 2. In benzene, DCM, acetone and DMA, EPR spectroscopy has shown that Co^{II}(salen) possesses a (d_{yz})²(d_{zx})²(d_{z²})²(d_{xy})¹(d_{x²-y²})⁰ electronic configuration,²⁴ thereby rationalising the inhibition of Co^{II}(salen) oxygenation at room temperature in these particular solvents. By contrast the (d_{yz})²(d_{zx})²(d_{xy})²(d_{z²})¹(d_{x²-y²})⁰ electronic configuration is present in coordinating solvents like pyridine,

dmsO and dmf.²⁴ MeOH has not been examined in this context *per se*, however, as a potentially coordinating solvent, and in the context of our observations that its presence is essential for the reactions where acetone, acetophenone and acetonitrile are the C–H substrates, it would seem likely that its axial coordination induces this electronic structure which is a pre-requisite for O₂ activation.

DFT calculations

Despite the wealth of experimental data available documenting the chemistry of Co(salen), this system has been scarcely addressed using DFT calculations.^{25–27} Crucially the mechanism of formation, and the reactivity of Co(salen)–O₂ adducts, have not been investigated. We have considered the routes to the organocobalt complexes, Co^{III}(salen)(CHRX) depicted in Scheme 3. The common starting point for all routes is the reaction of O₂ with Co^{II}(salen) (step i) to form the superoxide species Co^{III}(salen)(O₂[•])(MeOH) – the transient detected by EPR spectroscopy (Fig. 7a). Two alternative paths confront this species, reaction with the C–H of a substrate solvent molecule (step ii) or a second equivalent of Co^{II}(salen) (step v). In step ii, a hydrogen atom transfer (HAT) leads to the formation of a hydroperoxide complex Co^{III}(salen)OOH(MeOH), and the solvent-derived organic radical, [•]CHRX. From this point the final product, Co^{III}(salen)(CHRX)(MeOH), can be formed by either reaction of [•]CHRX with a second equivalent of Co^{II}(salen) (step iii) or the Co^{III}(salen)(OOH)(MeOH) can react with a second solvent molecule (step iv). The overall Co(salen): O₂ ratio would be 2 : 1.



Scheme 3 Alternative proposals for the mechanism of formation of organo Co(salen) complexes. Y is the number of product complexes relative to Co(salen); Y = 2 when following the left and middle path and Y = 4 when following the right. L = MeOH, MeNO₂ or EtNO₂. X = CN, COCH₃, COPh or NO₂ and R = H or CH₃.

An alternative route involves reaction of the initial, common $\text{Co}^{\text{III}}(\text{salen})(\text{O}_2^{\cdot-})(\text{MeOH})$ complex with a second equivalent of $\text{Co}^{\text{II}}(\text{salen})$ (step v) to give a peroxide-bridged complex $\{[(\text{MeOH})(\text{salen})\text{Co}^{\text{III}}]_2(\mu\text{-O}_2)\}$. There is structural precedence for such a complex (Scheme 2). Significantly, in the context of our results, DMSO, DMF, py or DMA with pyO were the solvents used in the preparations of these complexes.²³ Step vi shows the homolytic cleavage of the O–O bond in $\{[(\text{MeOH})(\text{salen})\text{Co}^{\text{III}}]_2(\mu\text{-O}_2)\}$ to produce two equivalents of $\text{Co}^{\text{IV}}(\text{salen})\text{O}(\text{MeOH})$ analogously to the proposal illustrated in Scheme 1B. Such a high-valent $\text{Co}^{\text{IV}}(\text{oxo})$ can be regarded as relatively inaccessible and therefore highly speculative. If it was generated, however, it might abstract a H atom from a C–H bond (step vii) and this would result in the formation of a solvent-derived organic radical, $\cdot\text{CHRX}$ and equimolar $\text{Co}^{\text{III}}(\text{salen})(\text{OH})(\text{MeOH})$. From here $\text{Co}^{\text{III}}(\text{salen})(\text{CHRX})(\text{MeOH})$ can be formed by either reaction of $\cdot\text{CHRX}$ with a second equivalent of $\text{Co}^{\text{II}}(\text{salen})$ (step viii) or $\text{Co}^{\text{III}}(\text{salen})(\text{OH})(\text{MeOH})$ can react with a second solvent molecule (step ix). The $\text{Co}(\text{salen})\text{:O}_2$ ratio that would be needed for this pathway is 4 : 1. As an alternative to the homolytic cleavage of $\{[(\text{MeOH})(\text{salen})\text{Co}^{\text{III}}]_2(\mu\text{-O}_2)\}$, this complex could also react directly with the solvent forming two equivalents of the final product $\text{Co}^{\text{III}}(\text{salen})(\text{CHRX})(\text{MeOH})$ (step x) and H_2O_2 . In this case the $\text{Co}(\text{salen})\text{:O}_2$ ratio required would be 2 : 1.

Fig. 8 shows the relative energy profile of the mechanism in which the common starting $\text{Co}^{\text{III}}(\text{salen})(\text{O}_2^{\cdot-})(\text{MeOH})$ reacts

with acetonitrile. Step i, the formation of $\text{Co}^{\text{III}}(\text{salen})(\text{O}_2^{\cdot-})(\text{MeOH})$, is exergonic. An axial MeOH ligand (not shown in Fig. 8) stabilises this superoxide complex: calculations show that $\text{Co}^{\text{III}}(\text{salen})(\text{O}_2^{\cdot-})$ is 23.2 kcal mol⁻¹ higher in energy compared to $\text{Co}^{\text{III}}(\text{salen})(\text{O}_2^{\cdot-})(\text{MeOH})$. An axial acetonitrile ligand ($\text{Co}^{\text{III}}(\text{salen})(\text{O}_2^{\cdot-})(\text{MeCN})$) results in a complex which is only 18.3 kcal mol⁻¹ lower in energy compared to $\text{Co}^{\text{III}}(\text{salen})(\text{O}_2^{\cdot-})$. Of the two possible spin states ($S = 1/2$ and $S = 3/2$) for $\text{Co}(\text{II})$ in $\text{Co}^{\text{II}}(\text{salen})$, that with the lowest energy is the low spin $S = 1/2$. The subsequent HAT (step ii) is endergonic by 27.9 kcal mol⁻¹, due to formation of an organic radical, resulting in a total energy slightly higher than the starting energy. That this increase in energy is caused by formation of a radical, is verified by the subsequent exergonic step iii (–40.6 kcal mol⁻¹) in which complexation of the radical by a second molecule of $\text{Co}^{\text{II}}(\text{salen})$ leads to the organocobalt complexes that have been isolated. By designating formation of H_2O_2 as the other product in step iv this process is endergonic. An exergonic process with a more complicated mechanism and production of O_2 and water is also feasible. For this, the $\text{Co}(\text{salen})\text{:O}_2$ ratio needed will be 4 : 1 and the energy of the final stage will be –52.9 kcal mol⁻¹ compared to –25.5 kcal mol⁻¹. We note that H_2O_2 can potentially participate in reactions which result in formation of additional $\text{Co}^{\text{III}}(\text{salen})(\text{CHRX})$ (eqn (1)–(4)):

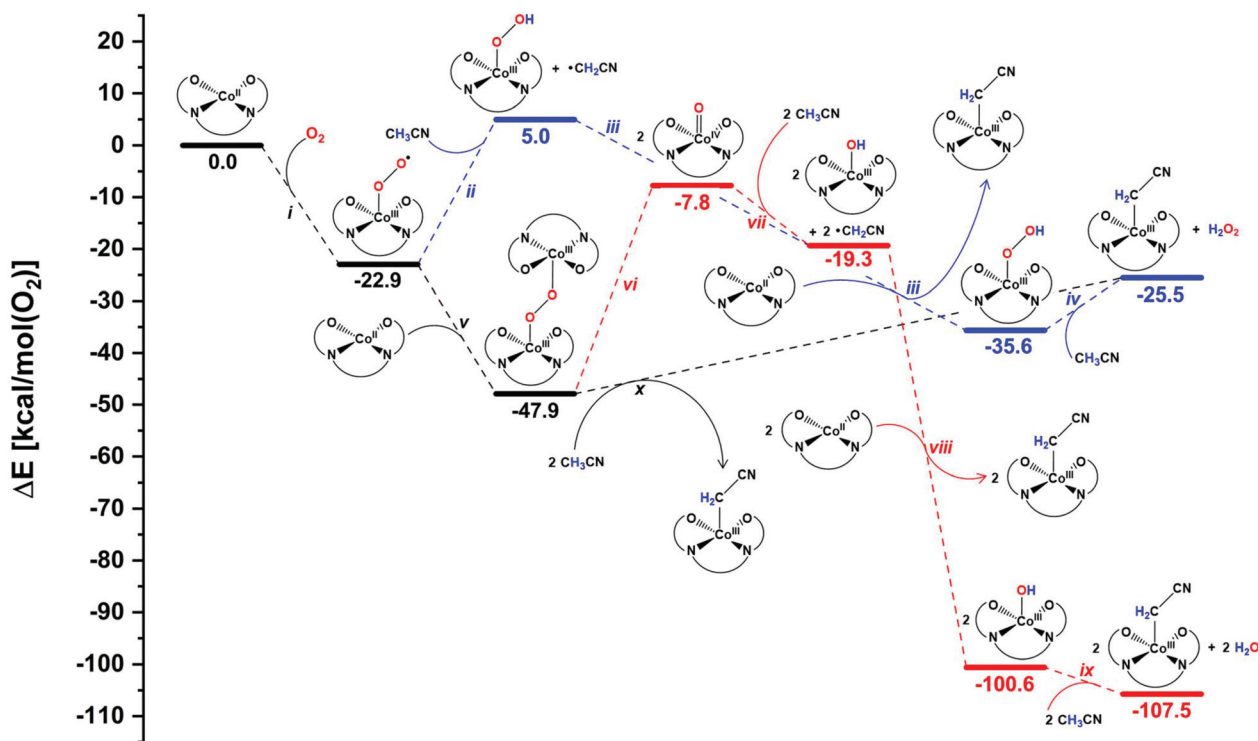
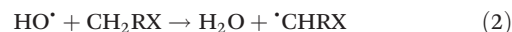
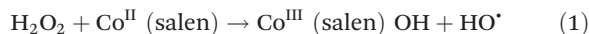
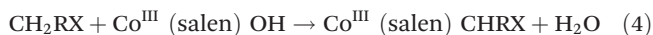


Fig. 8 Relative energy profile of the reaction mechanism in Fig. 7. The axial MeOH ligand, present on all complexes in the calculations with exception of $\text{Co}^{\text{II}}(\text{salen})$, is omitted for clarity. Note that the axis shows the energy difference per O_2 molecule. An acetonitrile solvent model was used for the calculations. $\text{Co}^{\text{II}}(\text{salen})$, $\text{Co}^{\text{III}}(\text{salen})\text{O}_2$ and $\text{Co}^{\text{IV}}(\text{salen})\text{O}$ are all $S = 1/2$.



Full conversion of $\text{Co}(\text{salen})$ would be achieved by reaction of $\text{Co}^{\text{III}}(\text{salen})\text{OH}$ with the solvent (eqn (4)). This is evidently possible for more acidic solvents like nitromethane and acetone.²⁸ This would also result in a $\text{Co}(\text{salen}) : \text{O}_2$ ratio of 4 : 1 and matches the mechanistic proposals made by Schaefer *et al.*⁹ who proposed that $\text{Co}(\text{III})$ superoxo or peroxo intermediates may attack the C–H bond of acetone.

The alternative pathway of $\text{Co}^{\text{III}}(\text{salen})(\text{O}_2\cdot)(\text{MeOH})$ reacting with a second $\text{Co}^{\text{II}}(\text{salen})$ and formation of a peroxide-bridged complex $\{[(\text{MeOH})(\text{salen})\text{Co}^{\text{III}}]_2(\mu\text{-O}_2)\}$ (step v) is computed to be more favorable than reaction with solvent (step ii). However, an onwards conversion by homolytic O–O cleavage to two $\text{Co}^{\text{IV}}(\text{salen})(\text{O})(\text{MeOH})$ complexes presents a very large barrier of 40.1 kcal mol⁻¹ (step vi); the most endergonic reaction considered according to the calculations. Of the three possible spin states ($S = 1/2$, $S = 3/2$ and $S = 5/2$) for $\text{Co}(\text{IV})$ in $\text{Co}^{\text{IV}}(\text{salen})(\text{O})(\text{MeOH})$, the $S = 1/2$ spin state is lowest in energy. Formation of $\text{Co}^{\text{IV}}(\text{salen})(\text{O})$ by a mononuclear mechanism through homolytic cleavage of $\text{Co}^{\text{III}}(\text{salen})(\text{OOH})(\text{MeOH})$ is also not energetically accessible: An energy state 157.2 kcal mol⁻¹ higher than the starting energy was obtained. By contrast, conversion of the $\{[(\text{MeOH})(\text{salen})\text{Co}^{\text{III}}]_2(\mu\text{-O}_2)\}$ to $\text{Co}^{\text{III}}(\text{salen})(\text{CHRX})(\text{MeOH})$ and H_2O_2 (step x) presents an energy barrier which is 22.4 kcal mol⁻¹ smaller than that for the homolytic O–O cleavage (step vi). Experimental verification of this pathway by H_2O_2 detection is however not possible since $\text{Co}^{\text{II}}(\text{salen})$ will immediately catalyse H_2O_2 disproportionation.

Despite being thermodynamically accessible according to the DFT calculations, $\{[(\text{MeOH})(\text{salen})\text{Co}^{\text{III}}]_2(\mu\text{-O}_2)\}$ could not be isolated from the reaction mixture. This suggests that kinetics plays a vital role in the outcome of the reaction. Step v can be viewed as an oxygen concentration dependent equilibrium, thus $\text{Co}^{\text{III}}(\text{salen})(\text{O}_2\cdot)(\text{MeOH})$ will be favoured at high oxygen concentrations, while $\{[(\text{MeOH})(\text{salen})\text{Co}^{\text{III}}]_2(\mu\text{-O}_2)\}$ favoured at low oxygen concentrations. Based on the mol fraction of oxygen available in the solvents used,²⁹ $\text{Co}(\text{salen}) : \text{O}_2$ ratios of between 1.5–2.5 : 1 can be expected at room temperature in air at ambient pressure. Solvent-reagent molecules will be available in up to 600-fold excess compared to $\text{Co}(\text{salen})$. Given that $\text{Co}^{\text{III}}(\text{salen})(\text{O}_2\cdot)(\text{MeOH})$ is likely to react with the first substrate it encounters, it is clearly far more likely to be a solvent molecule than a $\text{Co}(\text{salen})$. Reaction between $\text{Co}^{\text{III}}(\text{salen})(\text{O}_2\cdot)(\text{MeOH})$ and the solvent substrate will be essentially pseudo first order.

Even though the formation of $\{[(\text{MeOH})(\text{salen})\text{Co}^{\text{III}}]_2(\mu\text{-O}_2)\}$ is not kinetically favourable, and its homolytic CoO-OCo cleavage product, $\text{Co}^{\text{IV}}(\text{salen})(\text{O})(\text{MeOH})$, not favourable according to the calculations, for completeness we pursued computationally modelling the onward reaction of $\text{Co}^{\text{IV}}(\text{salen})(\text{O})(\text{MeOH})$. While a HAT from substrate to a hypothetical $\text{Co}^{\text{IV}}(\text{salen})(\text{O})(\text{MeOH})$ complex to give a $\text{Co}^{\text{III}}(\text{salen})(\text{OH})(\text{MeOH})$ (step vii) is exergonic, again predominantly due to the neutralisation of

$\cdot\text{CH}_2\text{CN}$ by reaction with excess $\text{Co}^{\text{II}}(\text{salen})$ (step viii), the product $\text{Co}^{\text{III}}(\text{salen})(\text{OH})(\text{MeOH})$ must then subsequently act as a base to deprotonate the incoming substituting MeCN (step ix, Scheme 3). In order to address the feasibility of this reaction, the pK_a of its conjugate acid, $[\text{Co}^{\text{III}}(\text{salen})(\text{OH}_2)(\text{MeOH})]^+$, was determined by calculation. This gave 3.32 in DMSO (8.50 in H_2O). The pK_a value of MeCN in DMSO is 31.3.³⁰ These data imply that the equilibrium constant for step ix can be estimated to $K \approx 10^{-28}$. Thus, despite the fact that calculations indicate step ix is exergonic by 6.9 kcal mol⁻¹, the very low predicted equilibrium constant suggests that it is not feasible for $\text{Co}^{\text{III}}(\text{salen})(\text{OH})(\text{MeOH})$ to act as a base for deprotonating the C–H bond of MeCN. In fact, this is consistent with experimental observations: $\text{Co}^{\text{III}}(\text{salen})\text{OH}$ stirred in MeCN at 10 °C for 48 hours does not result in reaction. If this solution is heated to 70 °C a reduction of the complex to $\text{Co}^{\text{II}}(\text{salen})$ occurs.³¹

To our knowledge only three transient $\text{Co}(\text{IV})$ oxo complexes, have been spectroscopically characterized.^{32–34} Interestingly, and in stark contrast to the reactions described here, one of these, $[(13\text{-TMC})\text{Co}^{\text{IV}}(\text{O})]^{2+}$, was characterized in solutions containing acetone, yet formation of an acetyl complex was not observed. HAT from C–H substrates with considerably lower BDEs of 73.7 kcal mol⁻¹ to 80.3 kcal mol⁻¹ were however achieved. The apparent differences in reactivity between $[(13\text{-TMC})\text{Co}^{\text{IV}}(\text{O})]^{2+}$ and the O_2 -activated $\text{Co}(\text{salen})$ is striking, pointing to different metal-based intermediates and therefore mechanisms for C–H oxidation.

Table 2 lists the bond dissociation energies (BDE), pK_a values and electron-pair donor ability (D_s) where available for the solvents used in this study. With C–H BDEs in the range 96.3–99.3 kcal mol⁻¹ and pK_a values ranging from 17.2 to 31.3, the solvents, in which the organometallic complexes form, are the least acidic of those that have been used in this and previous work. Notably, the D_s values are the largest for DMSO and DMF, solvents from which peroxide-bridged complexes have been isolated. The dependence on pK_a of the solvent suggest that the superoxide complex activates C–H bonds in the solvent molecule, and that this reaction has proton-transfer character.

In addition to consideration of the solvent properties in terms of its function as a substrate, its ability to activate $\text{Co}(\text{salen})$ towards oxygenation through axial coordination is also important. This can be expected to be influenced by sterics. Indeed, this is borne out through a comparison of the reactivity of $\text{Co}(\text{salen})$ towards O_2 in DMF vs. DMA. These two solvents have the same D_s value,³⁶ however, oxygenation (to produce a peroxide-bridged dimer) occurs only in DMF.²⁴ It is however possible the trap the peroxide-bridged complex in DMA if an axial donor ligand, whose π -acceptor properties are non-existent or very small, is added.²³ This is consistent with our observation that MeOH is needed in order to ultimately achieve formation of the organo $\text{Co}^{\text{III}}(\text{salen})$ complexes derived from acetonitrile, acetone and acetophenone.

The proposal in Scheme 1A¹¹ makes the assumption that it is the O–H bond in alcohols that is attacked by the $\text{Co}(\text{III})$ super-

Table 2 Bond dissociation energies (BDE), pK_a and electron-pair donor ability (D_s) for a selection of solvents

Solvent	Bond	BDE [kcal mol ⁻¹]	pK_a^a	D_s	Ref.
Nitromethane	CH ₃ NO ₂	99.3	17.2	9.0	30, 35 and 36
Nitroethane	CH ₃ CH ₂ NO ₂	98.1	16.7	—	30 and 35
Acetone	CH ₃ COCH ₃	96.0	26.5	15.0	35–37
Acetophenone	PhCOCH ₃	96.3	24.7	—	35 and 37
Acetonitrile	CH ₃ CN	97.0	31.3	12.0	30, 35 and 36
DMSO	CH ₃ S(O)CH ₃	94.0	35.1	27.5	30, 35 and 36
DMF	HCON(CH ₃) ₂	105.0	—	24.0	36 and 38
Methanol	CH ₃ OH	96.1	—	18.0	35 and 36
	CH ₃ OH	105.2	29.0	18.0	35, 36 and 39
TFE	CF ₃ CH ₂ OH	—	—	—	—
	CF ₃ CH ₂ OH	107.0	23.5	—	35 and 40
Water	H ₂ O	118.8	31.4	17.0	35, 36 and 39

^a Measured in DMSO, — not available.

oxo or peroxy species. This does not seem thermodynamically likely because the C–H bond next to the alcohol group has a significantly lower BDE compared with the O–H bond (Table 2). In light of our observations we posit that the mechanism for the formation of Co(salen) alkoxides from MeOH and 2,2,2-trifluoroethanol,^{5,11} involves similar initial steps to the formation of the organometallic complexes. Thus, direct O₂ activation, gives a superoxide intermediate followed by HAT from the alcohol C–H group. The product, Co(salen)(CHROH) (R = H, CF₃) is however not stable because of the α -hydroxyl group and this allows for facile rearrangement to the isolated Co(salen)(OCH₂R) complexes (Fig. 9a). DFT calculations (Fig. 9b) support the proposal that H atom removal from the

methylene C–H bond, rather than the alcohol O–H, is more favorable by 10.1 kcal mol⁻¹ and that O coordination in the final product is more favorable than C coordination by a 4.2 kcal mol⁻¹. It can be noted that the alkoxy complexes of Co(III)salen are sensitive to water and quantitatively converted to the corresponding hydroxy complexes when exposed to it. This contrasts to the organometallic complexes which are not hydrolysed.

Conclusions

Co(III)salen superoxo and peroxy complexes have benchmarked the ways in which O₂ can bind to transition metal ions the superoxo complexes have been shown to oxidize C–H bonds of co-ligands,⁴¹ and external organic substrates.^{22,42,43} We show also that the pK_a value of the C–H bond of the terminal methyl groups the solvent media is critical for whether or not an O₂ adduct is stable, or whether it reacts further to give an organometallic complex. In turn, the stability of the organometallic product can be compromised by the group α to the coordinated carbon. We have presented a unifying mechanistic link between the formation of diverse, and in some cases, landmark peroxy, superoxo, organocobalt and alkoxide complexes of Co(III)salen.

A central question has been the identity of intermediate cobalt-based oxidant(s) for C–H oxidation formed by the activation of O₂ by Co(salen). Is this a Co(III)-superoxide, a dimeric Co(III)₂- μ -peroxide or a Co(IV)oxo intermediate? Our results point to the Co(III)-superoxide species at that which attacks C–H bonds under kinetic control. Thus, the initial stages are similar to pathway A in Scheme 1 – however it is C–H bonds of solvents, including alcohols (*i.e.* not their O–H bonds) that are susceptible to attack. The Co(III)₂- μ -peroxide is relatively stable, if formed, but may also be able to activate C–H bonds under appropriate conditions. We find no support for the involvement of a Co(IV)oxo species. In this context we note also that HAT from acetonitrile has not been observed for high-valent Fe(IV)oxo complexes where this solvent is used as the media for their formation.^{44–47}

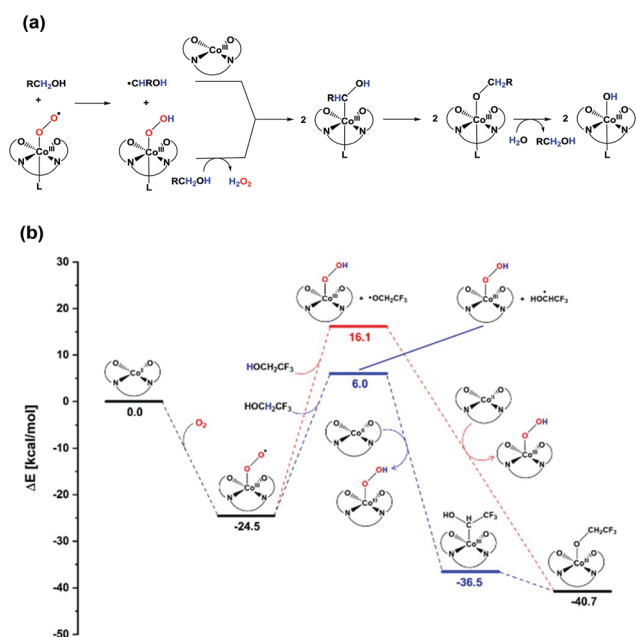


Fig. 9 (a) Proposed mechanism for formation of Co(salen) alkoxides, L = RCH₂OH. (b) Relative energy profile for the reaction between Co(salen) and CF₃CH₂OH. The axial CF₃CH₂OH ligand, present on all complexes in the calculations with exception of Co(III)salen, is omitted for clarity.

Author contributions

M.S.M. synthesized the compounds, performed the measurements, processed and analyzed the experimental and computational data, prepared the original draft and designed the figures. J.K. supervised the computational work. C.J.M. conceived and supervised the work, managed resources and acquired funding. M.S.M. and C.J.M. wrote the manuscript in consultation with J.K.

Conflicts of interest

There are no conflicts to declare.

Acknowledgements

The work was supported by the Danish Council for Independent Research (Grant 9041-00170B) and the Carlsberg Foundation grant CF15-0675 for the X-ray diffractometer. Professor Vickie McKee is thanked for advice on the crystal structure determinations. Professor Ulla Gro Nielsen is thanked for helpful discussions regarding the SSNMR spectra.

Notes and references

- C. Floriani, M. Puppis and F. Calderazzo, *J. Organomet. Chem.*, 1968, **12**, 209–223.
- D. R. Chambers, R. E. Sullivan and D. B. C. Martin, *Organometallics*, 2017, **36**, 1630–1639.
- N. A. Bailey, B. M. Higson and E. D. McKenzie, *Inorg. Nucl. Chem. Lett.*, 1971, **7**, 591–593.
- Y. Fujii and T. Yoshizawa, *Chem. Lett.*, 1976, **5**, 117–120.
- M. Cesari, C. Neri, G. Perego, E. Perrotti and A. Zazzetta, *J. Chem. Soc. D*, 1970, 276–277.
- C. Neri and E. Perrotti, US3787464A, 1974.
- R. S. Gall, J. F. Rogers, W. P. Schaefer and G. G. Christoph, *J. Am. Chem. Soc.*, 1976, **98**, 5135–5144.
- W. P. Schaefer, B. T. Huie, M. G. Kurilla and S. E. Ealick, *Inorg. Chem.*, 1980, **19**, 340–344.
- W. P. Schaefer, R. Waltzman and B. T. Huie, *J. Am. Chem. Soc.*, 1978, **100**, 5063–5067.
- R. H. Bailes and M. Calvin, *J. Am. Chem. Soc.*, 1947, **69**, 1886–1893.
- A. Nishinaga, T. Kondo and T. Matsuura, *Chem. Lett.*, 1985, **14**, 905–908.
- A. I. Nguyen, R. G. Hadt, E. I. Solomon and T. D. Tilley, *Chem. Sci.*, 2014, **5**, 2874–2878.
- K. L. Brown, S. Cheng, X. Zou, J. Li, G. Chen, E. J. Valente, J. D. Zubkowski and H. M. Marques, *Biochemistry*, 1998, **37**, 9704–9715.
- T. G. Pagano, L. G. Marzilli, M. M. Flocco, C. Tsai, H. L. Carrell and J. P. Glusker, *J. Am. Chem. Soc.*, 1991, **113**, 531–542.
- S. Brückner, M. Calligaris, G. Nardin and L. Randaccio, *Acta Crystallogr., Sect. B: Struct. Crystallogr. Cryst. Chem.*, 1969, **25**, 1671–1674.
- L. E. Sutton and H. J. M. Bowen, *Tables of Interatomic Distances and Configuration in Molecules and Ions*, 1958.
- NIST Chemistry WebBook*, <https://webbook.nist.gov/chemistry/>, (accessed May 26, 2019).
- G. Costa, G. Mestroni, G. Tazzer and L. Stefani, *J. Organomet. Chem.*, 1966, **6**, 181–187.
- D. Doddrell and A. Allerhand, *Proc. Natl. Acad. Sci. U. S. A.*, 1971, **68**, 1083–1088.
- V. Balzani, L. Moggi, F. Scandola and V. Carassiti, *Inorg. Chim. Acta Rev.*, 1967, **1**, 7–34.
- B. M. Hoffman, D. L. Diemente and F. Basolo, *J. Am. Chem. Soc.*, 1970, **92**, 61–65.
- A. Nishinaga, H. Tomita, K. Nishizawa, T. Matsuura, S. Ooi and K. Hirotsu, *J. Chem. Soc., Dalton Trans.*, 1981, 1504.
- C. Floriani and F. Calderazzo, *J. Chem. Soc. A*, 1969, 946.
- E. Ochiai, *J. Chem. Soc., Chem. Commun.*, 1972, 489–490.
- N. J. Henson, P. J. Hay and A. Redondo, *Inorg. Chem.*, 1999, **38**, 1618–1626.
- A. Kochem, H. Kanso, B. Baptiste, H. Arora, C. Philouze, O. Jarjayes, H. Vezin, D. Luneau, M. Orio and F. Thomas, *Inorg. Chem.*, 2012, **51**, 10557–10571.
- A. G. Starikov, V. I. Minkin and A. A. Starikova, *Struct. Chem.*, 2014, **25**, 1865–1871.
- A. Bigotto, G. Costa, G. Mestroni, G. Pellizer, A. Puxeddu, E. Reisenhofer, L. Stefani and G. Tazzer, *Inorg. Chim. Acta Rev.*, 1970, **4**, 41–49.
- Oxygen and Ozone: Solubility Data Series (Volume 7)*, ed. R. Battino, Pergamon, 1981.
- W. S. Matthews, J. E. Bares, J. E. Bartmess, F. G. Bordwell, F. J. Cornforth, G. E. Drucker, Z. Margolin, R. J. McCallum, G. J. McCollum and N. R. Vanier, *J. Am. Chem. Soc.*, 1975, **97**, 7006–7014.
- K. Aoki and S. Minami, US4746748A, 1988.
- B. Wang, Y.-M. Lee, W.-Y. Tcho, S. Tussupbayev, S.-T. Kim, Y. Kim, M. S. Seo, K.-B. Cho, Y. Dede, B. C. Keegan, T. Ogura, S. H. Kim, T. Ohta, M.-H. Baik, K. Ray, J. Shearer and W. Nam, *Nat. Commun.*, 2017, **8**, 14839.
- F. F. Pfaff, S. Kundu, M. Risch, S. Pandian, F. Heims, I. Pryjomska-Ray, P. Haack, R. Metzinger, E. Bill, H. Dau, P. Comba and K. Ray, *Angew. Chem., Int. Ed.*, 2011, **50**(7), 1711–1715.
- S. Hong, F. F. Pfaff, E. Kwon, Y. Wang, M. Seo, E. Bill, K. Ray and W. Nam, *Angew. Chem., Int. Ed.*, 2014, **53**(39), 10403–10407.
- Y.-R. Lou, *Comprehensive Handbook of Chemical Bond Energies*, CRC Press, 2007.
- M. Sandström, I. Persson, P. Persson, E. K. Euranto, T. Brekke, D. W. Aksnes and T. Tokii, *Acta Chem. Scand.*, 1990, **44**, 653–675.

- 37 F. G. Bordwell and J. A. Harrelson Jr., *Can. J. Chem.*, 1990, **68**, 1714–1718.
- 38 Y.-R. Luo, *Comprehensive handbook of chemical bond energies*, CRC Press, 2007.
- 39 W. N. Olmstead, Z. Margolin and F. G. Bordwell, *J. Org. Chem.*, 1980, **45**, 3295–3299.
- 40 L. M. Huffman, A. Casitas, M. Font, M. Canta, M. Costas, X. Ribas and S. S. Stahl, *Chem. – Eur. J.*, 2011, **17**, 10643–10650.
- 41 M. S. Vad, A. Nielsen, A. Lennartson, A. D. Bond, J. E. McGrady and C. J. McKenzie, *Dalton Trans.*, 2011, **40**, 10698–10707.
- 42 A. Nishinaga, H. Tomita, M. Oda and T. Matsuura, *Tetrahedron Lett.*, 1982, **23**, 339–342.
- 43 T. Corona, S. K. Padamati, F. Acuña-Parés, C. Duboc, W. R. Browne and A. Company, *Chem. Commun.*, 2017, **53**, 11782–11785.
- 44 R. Singh, G. Ganguly, S. O. Malinkin, S. Demeshko, F. Meyer, E. Nordlander and T. K. Paine, *Inorg. Chem.*, 2019, **58**, 1862–1876.
- 45 J. P. Bigi, W. H. Harman, B. Lassalle-Kaiser, D. M. Robles, T. A. Stich, J. Yano, R. D. Britt and C. J. Chang, *J. Am. Chem. Soc.*, 2012, **134**, 1536–1542.
- 46 C. Wegeberg, W. R. Browne and C. J. McKenzie, *ACS Catal.*, 2018, **8**, 9980–9991.
- 47 J.-U. Rohde, J.-H. In, M. H. Lim, W. W. Brennessel, M. R. Bukowski, A. Stubna, E. Münck, W. Nam and L. Que, *Science*, 2003, **299**, 1037–1039.